Corrosion Science 74 (2013) 194–205

Contents lists available at SciVerse ScienceDirect

Corrosion Science

journal homepage: www.elsevier.com/locate/corsci

Painting rusted steel: The role of aluminum phosphosilicate

S.N. Roselli, B. del Amo, R.O. Carbonari, A.R. Di Sarli, R. Romagnoli *

CIDEPINT. Centro de Investigación y Desarrollo en Tecnología de Pinturas, Calle 52 e/121 y 122, 1900 La Plata, Argentina

ARTICLE INFO

Article history:
Received 26 December 2012
Accepted 25 April 2013
Available online 14 May 2013

Keywords:
A. Organic coatings
A. Steel
B. EIS
B. SEM
C. Rust
C. Paint coatings

ABSTRACT

Surface preparation is a key factor for the adequate performance of a paint system. The aim of this investigation is to employ a wash-primer to accomplish the chemical conversion of rusted surface when current cleaning operations are difficult to carry out. The active component of the wash-primer was aluminum phosphosilicate whose electrochemical behavior and the composition of the generated protective layer, both, were studied by electrochemical techniques and scanning electron microscopy (SEM), respectively. Primed rusted steel panels were coated with an alkyd system to perform accelerated tests in the salt spray chamber and electrochemical impedance measurements (EIS). These tests were conducted in parallel with a chromate wash primer and the same alkyd system. Results showed that the wash-primer containing aluminum phosphosilicate could be used satisfactorily to paint rusted steel exhibiting a similar performance to the chromate primer.

1. Introduction

Surface preparation is a key factor prior to painting and the success of the protective paint system depends on its correct execution. Poor surface preparation followed by a good paint system usually brings worse results than the use of low quality products on a well prepared surface.

One of the major factors affecting the paint system performance is the presence of soluble salts at the paint metal interface. It is known that the presence of water soluble species, mainly chlorides and sulfates, at the metal/paint interface, promotes osmotic blistering of the coating and underfilm metallic corrosion when the concentration exceeds a critical level. Both processes can lead to the deterioration of the paint system in a very short period of time. However, it is difficult to set acceptable unique levels since each type of coating varies in susceptibility to soluble salt degradation which also depends on both coating thickness and the exposure conditions [1].

The other factor that may influence negatively the behavior of a paint system is the presence of oxides on the metal surface. Manual cleaning to prepare surfaces for coating may be accomplished by brushing, scraping or abrading the metal surface to remove rust, mill scale or slightly adhering old paint. It is slow and laborious but often used when it is not possible to employ other methods such as sand or grit blasting. It is recommended in the case of difficulties to access certain region of the pieces, complicated configuration or very high cost cleaning operations. Blasting operations may be risky to the operator and, at the same time, contaminate the environment. Mechanical cleaning requires of devices such as wire brushes, air guns, impact grinders, and abrading discs. Both manual and mechanical cleaning do not completely eliminate rust or scale and subsequent painting brings serious problems such as lack of adherence of the coating system to the base metal.

The effect of remaining oxides and different degrees of surface preparation on the performance of the coating system was studied by different authors through outdoor exposure tests and electrochemical essays [2,3]. They found that the most corrosion resistant surfaces were those primed with inorganic zinc rich paints. The same conclusion was obtained with epoxy paints and paints pigmented with red lead which was banned [3]. In many cases it was found that the influence of the presence of surface oxides on the performance of the coating system was negligible.

When it is not possible to eliminate oxides or the mill scale by blasting, the chemical conversion of the surface is the recommended method. A conversion coating may be defined as one formed by a chemical reaction which converts the surface of a metal substrate into a compound which became part of the coating. The primer designed in this research is aimed to generate conversion films [4–6].

The formation of a stable conversion layer is mandatory to ensure the adequate performance of the paint system; particularly during wetting and drying of steel surfaces exposed to the atmosphere. In these cases corrosion potential also changes periodically with time and rust formed on the steel modifies its nature by phase transformations [7–11]. In addition, several cations coming from the paint components can migrate into the oxide layer to be incorporated in the iron oxide lattice [12,13]. As a consequence, strong

* Corresponding author. Tel.: +54 221 483 1142.
E-mail address: estelectro@cidepint.gov.ar (R. Romagnoli).

0010-938X/$ - see front matter © 2013 Elsevier Ltd. All rights reserved.
http://dx.doi.org/10.1016/j.corsci.2013.04.043

changes in the corrosion behavior are to be expected [14]. These cations may act either on the dry or on the wet cycle. For instance, chromium may decrease the corrosion rate during drying, presumably by inhibiting the cathodic reaction [15].

Tannins were normally used to convert the steel surfaces because they react with the remaining iron oxides, in the presence of phosphoric acid, to form iron "tannates" [16–20]. Several types of tannins, from different trees, were employed. The most widespread ones were extracted from the following plants: mimosa [21–24], chestnut [25,26], pine [27], "quebracho" [28], mangrove [29,30], etc. Results obtained with the use of tannins are controversial although, as a general rule, when applied on corroded substrates they improve the corrosion behavior of the coating system [26,31,32].

More recently, self-priming and surface-tolerant paints were developed. These paints incorporate phosphoric acid in their formulation to react with one of its components, polyvinyl alcohol, to form an ester. The ester diffuses into the oxide layer when moisture penetrates the paint film and transforms the different phases of iron oxide in a stable one constituted by maghemite. The transformed oxide layer strongly adheres to the binder through O–P–O bond to form, in this way, a passivating layer which improves the corrosion resistance of the paint [33,34].

The objective of this research was to modify a chromate based wash primer and study its performance on rusted SAE 1010 steel substrates. Zinc tetroxychromate was replaced by aluminum phosphosilicate, synthesized in the laboratory. Aluminum phosphosilicate combines two inhibitive species, the phosphate anion and the silica particle. The anti-corrosion behavior of aluminum phosphosilicate was studied by electrochemical techniques, particularly linear polarization experiments. The corrosion behavior of steel primed and painted with an alkyd system was evaluated in the salt spray chamber and by electrochemical impedance measurements (EIS). In both cases, electrochemical measurements were supplemented with observations by scanning electron microscopy (SEM).

2. Experimental section

2.1. Precipitation curves

Different solutions were prepared so that it was possible to study the acid–base and precipitation equilibria in systems consisting of the reagents used in the synthesis of aluminum phosphosilicate: SiO_2, H_3PO_4 and Al^{3+}. The composition of the titrated solutions may be found in the caption of Fig. 1. The acid–base equilibrium of each reagent was studied firstly. Then, the same study was carried out employing the aforementioned reagents but combined in pairs and, finally, all three together. Except for the sodium silicate solution, the remainder systems were acidified with hydrochloric acid to bring the pH below 1.20 to observe changes occurring with increasing pH, which finally, should lead to the precipitation of aluminum phosphosilicate. The titrant was 0.5000 M sodium hydroxide. Due to its alkaline nature, the sodium silicate solution was titrated with hydrochloric acid of the same concentration as the sodium hydroxide employed as titrant. The titrations were made following the procedures described in the literature [35,36].

2.2. The synthesis of aluminum phosphosilicate

In the first instance, a sodium silicate solution was prepared employing Aerosil 200®, a nanometric silica, whose particle size ranged between 12 and 16 nm and its specific surface area was 200 $m^2\ g^{-1}$. The solution was obtained by dissolving 0.6000 g of this silica in 100 mL of distilled water containing 0.800 g of sodium hydroxide. Then, the pH was lowered to 1.2 with phosphoric acid. Finally, 3.75 g of aluminum nitrate nonahydrate we added to the colloidal dispersion to precipitate the aluminum phosphosilicate. The addition of the reagents was performed with constant stirring of 300 rpm. The resulting system was allowed to stand for 24 h and the pH was adjusted to 3.5 using a glass electrode and 0.50 M NaOH.

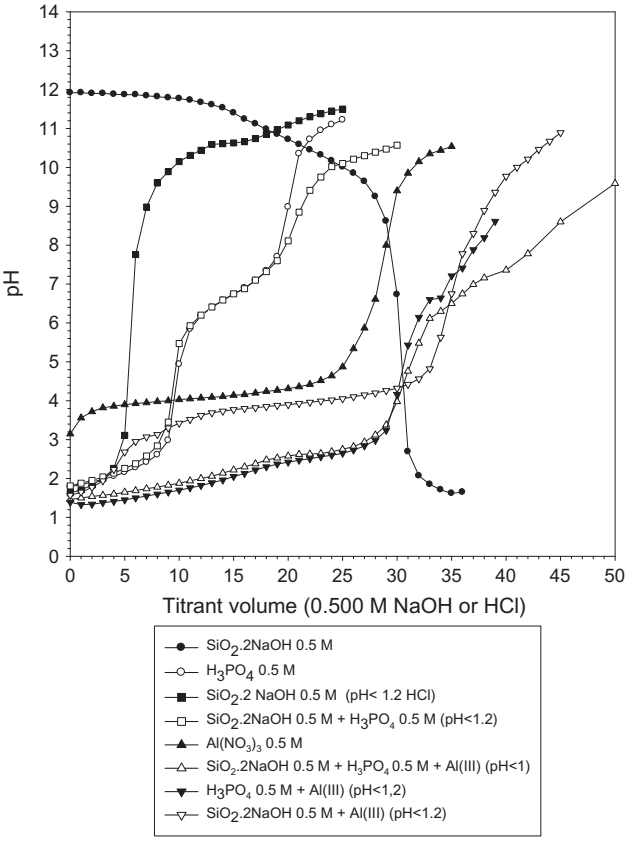

Fig. 1. Study of acid–base and precipitation equilibria of the reactants employed to synthesize aluminum phosphosilicate.

Once the precipitate was obtained, it was vacuum filtered through a Büchner funnel with medium pore filter paper (Whatman 40 or similar), air dried and milled to pass through the sieve No. 20. Finally, the precipitate was dried at 50 °C until constant weight.

The solid obtained as described before was characterized by conventional analytical techniques and by FTIR spectroscopy, preparing a potassium bromide pellet, with a Perkin Elmer SPECTRUM ONE spectrometer.

2.3. Study of reaction products between aluminum phosphosilicate and iron oxides

The nature of the reaction products between the aluminum phosphosilicate and the oxides naturally grown on a SAE 1010 steel panel was studied employing a mixture containing the oxides and the pigment in a molar ratio: 2:1. The oxides were scraped up from steel panels rusted in the laboratory atmosphere (20 ± 2 °C, RH 70%) during 2 years and they were characterized by FTIR spectroscopy. The mixture was left in the laboratory environment during 15 days, wetting it periodically with distilled water. After this period, it was dried at 100 ± 5 °C to constant weight just to eliminate free water to obtain the FTIR spectrum employing a potassium

bromide pellet. Free water must be eliminated because its enhanced absorption bands could shield other bands present in the spectrum.

2.4. Electrochemical characterization of aluminum phosphosilicate

The anti-corrosion behavior of aluminum phosphosilicate was assessed by electrochemical techniques. The cell to perform corrosion potential (E_{corr}) measurements had two electrodes; a rusted steel panel (area: 4 cm^2) and the saturated calomel electrode (SCE) as reference. The electrolyte was an aluminum phosphosilicate suspension in 0.025 M NaCl. Once the corrosion potential measurement had finished, panels were removed from the suspension, washed thoroughly with distilled water, acetone and dried. The surface, as mentioned above, was observed by SEM using a brand microscope FEI Quanta 200 with tungsten filament. The surface elemental composition of the protective film was obtained with an energy dispersive RX microanalyzer end the EDX detector Apollo 40.

Corrosion rates were determined by the polarization resistance technique [37–39] employing the Potentiostat–Galvanostat EG&G PAR Model 273A and a conventional three electrode cell. The working electrode was the rusted steel panel (area: 1 cm^2), the reference was the SCE and the counterelectrode a Pt mesh. The supporting electrolyte was similar to that employed in corrosion potential measurements but with 0.1 M NaCl. The sweep amplitude was ±20 mV o.c. and the scan rate 0.1661 mV s^{-1}. All electrochemical measurements were carried out in normally aerated stirred solutions (300 rpm).

2.5. Preparation and application of the wash-primer with aluminum phosphosilicate and the alkyd paint system

The wash primer was prepared on the basis of the chromate formulation reported in Table 1. Part A of the wash primer was prepared by dispersing the components in a ball mill during 24 h. The active components of the primer were basic zinc chromate and phosphoric acid. The film forming material was the polyvinyl butyral resin [40]. The volume fraction of basic zinc chromate was replaced by aluminum phosphosilicate to formulate the alternative wash primer. Aluminum phosphosilicate was prepared according to the procedure described previously. Prior to painting, rusted panels were hand brushed with a wire brush and abraded with No. 100 emery paper. The primer was applied by brushing on steel panels, previously degreased with toluene, to match a final dry film thickness of 7 ± 1 μm. In spite of the application method, the dispersion obtained for the film thickness was not so high due to the low viscosity of the formulation and its great ability to flow.

Table 1
Chromate based wash primer pre-treatment according to SSPC-PT 3–64 standard specification.

Part A		Part B	
Component	wt%	Component	wt%
Polyvinyl butyral resin $(C_8H_{14}O_2)_n$	9.2	Phosphoric acid (85%)	18.5
Basic zinc chromate $ZnCrO_4{\cdot}4Zn(OH)_2{\cdot}H_2O$	8.8	Isopropanol	16.2
Magnesium silicate $3MgO{\cdot}4SiO_2{\cdot}H_2O$	1.3	Water (maximum)	65.3
Carbon black	0.1		
n-Buthanol $C_4H_{10}O$	20.5		
Isopropanol C_3H_8O	57.7		
Water (maximum)	2.4		

Mixing ratio: 4 parts of A by weight + 1 part of B.

The panels were allowed to stand for 7 days before testing.

2.6. Characterization of the protective layer formed beneath the primer by SEM

The morphology and surface elemental composition of the protective layer generated by the application of the primer, both were studied by SEM and EDX analysis, respectively. The primers were applied on rusted panels, allowed to react with the base metal during 14 days and finally removed with a suitable solvent mixture.

2.7. Accelerated tests and electrochemical essays on painted panels

Primed panels were subjected to different assays. Anodic and cathodic polarization curves of rusted steel and the primed samples were obtained at different immersion times, during 24 h, employing a three electrodes cell. The working electrode was the rusted steel, the SCE was used as reference and a platinum grid was the counter-electrode. The supporting electrolyte was 0.1 M NaCl. The sweep began in the vicinity of the corrosion potential at a scan rate of 3 mV s^{-1}. As no significant differences were noted between 0.5 and 3 mV s^{-1}, this rather high scan rate was adopted for the sake of simplicity. Experiments were run on defect-free coatings. Measurements were carried out with a Potentiostat–Galvanostat EG&G PAR Model 273A plus SOFTCORR 352 software. These voltammetric experiments were possible due to the low ohmic drop of the primers 0.50–0.70 kΩ cm^2 [41].

Panels submitted to the salt spray chamber and those appointed for electrochemical impedance spectroscopy, both sets were further coated with a protective paint and a topcoat; each one 35 μm dry film thickness. The composition of the protective paint, expressed as percentage by weight, was as follows: zinc "molybdenum" phosphate, 14.1%; nonfibrous magnesium silicate ($3MgO{\cdot}4SiO_2{\cdot}H_2O$), 10.6%; barite ($BaSO_4$), 18.6%; titanium dioxide (TiO_2), 6.7; alkyd resin/"white spirit" (1:1), 40.6% and toluene (C_7H_8), 9.4%. Zinc "molybdenum" phosphate is a white anticorrosion pigment which contained 1.6% of zinc molybdate ($ZnMoO_4$) and 98.4% of zinc phosphate ($Zn_3(PO_4)_2{\cdot}4H_2O$). "White spirit" is a typical solvent for alkyd paints and it consists of a mixture of aliphatic and alicyclic C7 to C12 hydrocarbons with a maximum content of 25% of C7 to C12 aromatic hydrocarbons. The topcoat was a commercial alkyd paint pigmented with titanium dioxide whose pigment volume concentration was 18.0%.

A set of three panels was placed in the salt spray chamber (ASTM B-117). Rusting (ASTM D-610) and blistering (ASTM D-714) degrees were evaluated after 3050 h of exposure. The adhesion of coatings to steel substrate was also measured by the cross-cut tape test (ASTM D 3359), periodically, during the exposure in the salt spray chamber.

Impedance spectra of painted panels (frequency range 1.10^5 - Hz $\leqslant f \leqslant 1 \times 10^{-2}$ Hz) were performed in the potentiostatic mode, at the E_{corr}. Measurements were carried out as a function of the exposure time in 3% NaCl, using the 1255 Solartron FRA and the 1286 Solartron EI. The amplitude of the applied AC voltage was 0.010 V peak to peak. Two acrylic tubes were attached to each coated panel (working electrode) with an epoxy adhesive; the geometric area exposed to the electrolyte in each cell was 15.9 cm^2. A large area Pt–Rh mesh of negligible impedance and the SCE were employed as auxiliary and reference electrodes, respectively. The experimental impedance spectra were interpreted on the basis of equivalent electrical circuits using a suitable fitting procedure developed by Boukamp [42]. This electrochemical experiments were carried out at laboratory temperature (20 ± 2 °C), using a Faraday cage. Simultaneously, corrosion potential values were recorded as a function of immersion time.

3. Results and discussion

3.1. Precipitation curves

The analysis of the titration curves of Fig. 1 showed that no significant changes took place with respect to the formation of new phases in the titration of the sodium silicate solution acidified with hydrochloric acid. Only a sudden pH increase was observed at the beginning of the titration. Something similar was found to occur on titrating the solution containing alkaline sodium silicate. In both cases, at pH ~ 10.9, it was observed a small inflection in the titration curve that could be associated with a change in the structure of the colloidal sodium silicate solution.

The titration of phosphoric acid did not change significantly by the presence of silica, at least in the region of pH < 7. However, noticeable differences between the two curves were observed at pH > 7 probably due to hydrolysis of siliceous and/or aluminum compounds that might have co-precipitated with the phosphate. The precipitation curves of aluminum hydroxide and aluminum phosphate presented a conventional shape. In change, the titration curve of aluminum phosphate changed in the presence of sodium silicate from the titration end point on, probably due to the alkaline hydrolysis of a fraction of the solid phase (the siliceous and/or aluminum compounds). In addition, there was clear evidence that a compound between silica and aluminum formed at a lower pH than that corresponding to the precipitation of aluminum hydroxide.

The analysis of the precipitate, by current analytical techniques, showed that the composition of aluminum phosphosilicate was Al $(SiO_2)_{1.5}$ PO_4, close to the theoretical one, as reported in the literature [43,44]. As no differences were found between the precipitation of aluminum phosphate and aluminum phosphosilicate, according to precipitation curves, but the behavior of both compounds differed in the alkaline region; it was thought that the silica fraction co-precipitated with aluminum phosphate. As it would be pointed out later this fraction resulted protonated. The FTIR spectrum of the precipitated solid had the characteristic band corresponding to the stretching of the phosphate anion bonds in the region of 1000–1100 cm^{-1}. The main band corresponding to silica superimposed with this band. The band between 500 and 600 cm^{-1} can be assigned to the twisting of P–O bonds [45,46]. Phosphosilicates also exhibit characteristic bands at ~917 cm^{-1} which corresponded to the stretching of the Si–O bond. The absorption band 1640 cm^{-1} could be associated with the vibration of the H–O–H bond of associated molecular water (Fig. 2). Finally, the band at 1385 cm^{-1} may be attributed to nitrate ion which was thought to act as the counterion of protons in the silica fraction of the aluminum phosphosilicate.

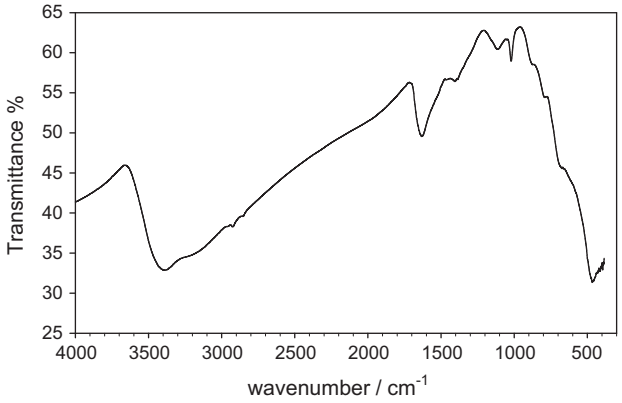

Fig. 3. FTIR spectrum of oxides grown on a SAE 1010 steel panel in the laboratory atmosphere (20 ± 2 °C, RH 70%).

3.2. Study of reaction products between aluminum phosphosilicate and iron oxides

The oxide naturally grown on a steel panel in the laboratory atmosphere was analyzed by FTIR spectroscopy (Fig. 3) and it was found to consist of a hydrated mixture of lepidocrosite, feroxihite and ferrihydrite. Lepidocrosite possess typical absorption bands at 742 and 1020 cm^{-1} while feroxihite exhibits absorption bands at 477 cm^{-1}. The bands corresponding to ferrihydrite may be found at 463, 539 and 1384 cm^{-1} [47,48]. The comparison of the aluminum phosphosilicate spectrum (Fig. 2) with that of the reaction products between this pigment and the iron oxides (Fig. 4) showed that oxides were phosphatized and oxide typical IR bands disappeared. Both spectra were very similar but a shift in the absorption maximum at 1000 cm^{-1} was detected and this could indicate, probably, a change in the chemical structure of the phosphate. No band was observed at 1380 cm^{-1} which appeared in the FTIR spectrum of the aluminum phosphosilicate.

3.3. Electrochemical characterization of aluminum phosphosilicate

Steel corrosion potential in the aluminum phosphosilicate suspension was ~650 mV vs. SCE, during the whole test period. This value is consistent with the formation of an oxide layer that was partially stabilized or converted into the corresponding phosphate.

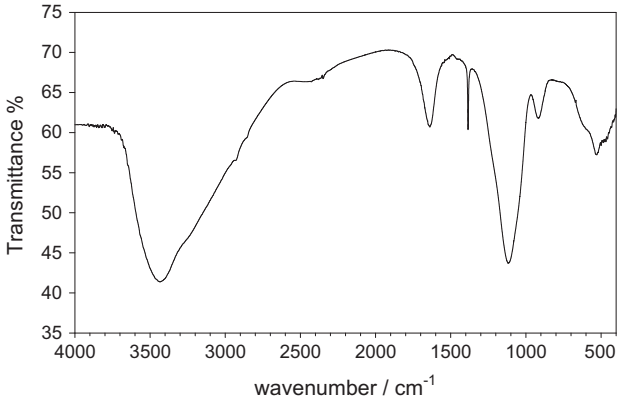

Fig. 2. FTIR spectrum of aluminum phosphosilicate.

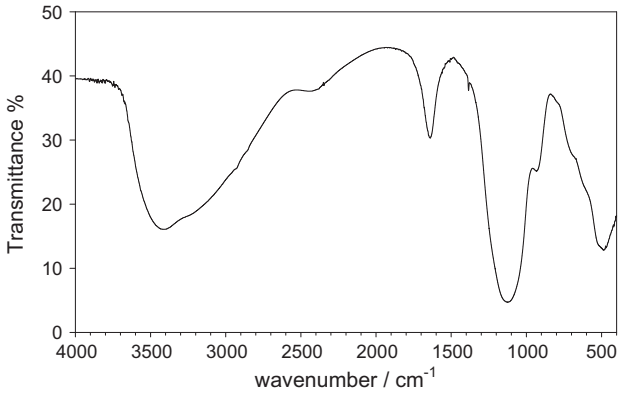

Fig. 4. FTIR spectrum of the reaction products between iron oxides and aluminum phosphosilicate.

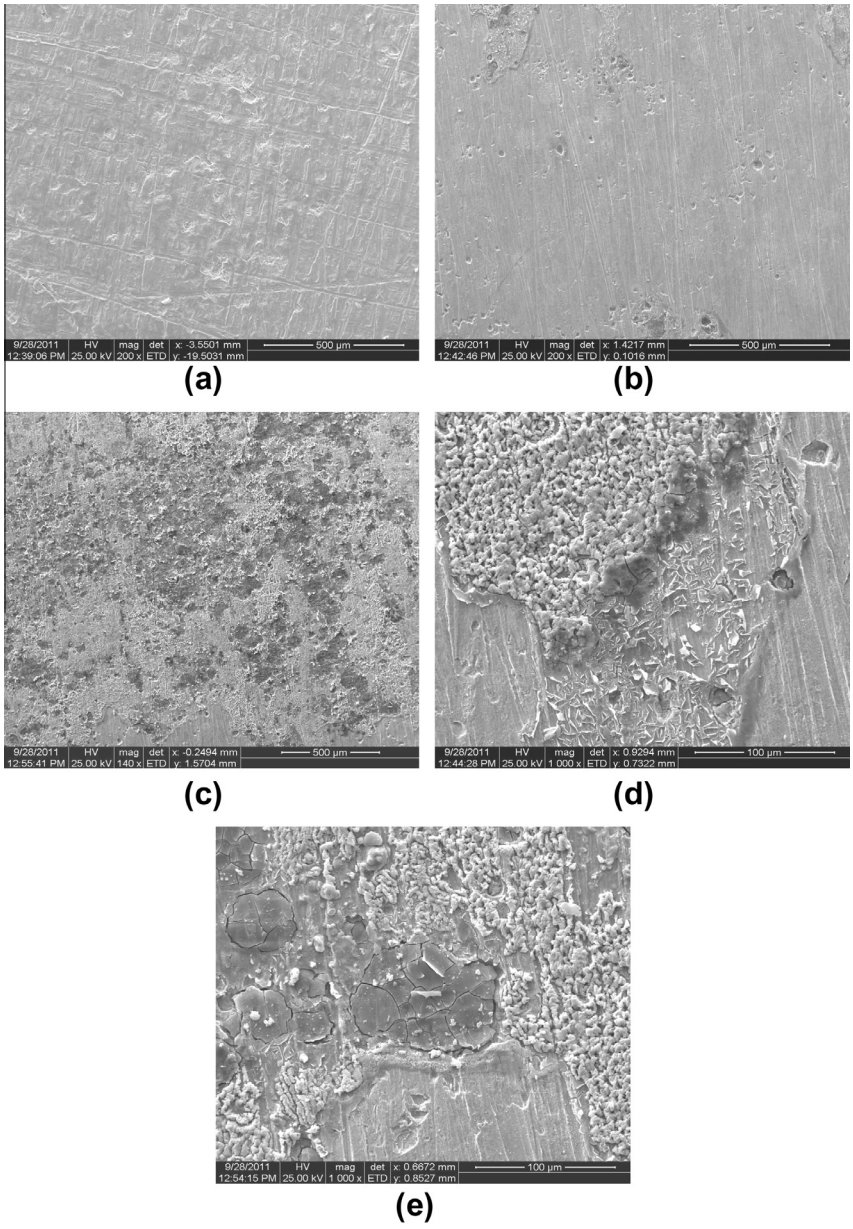

Fig. 5. SEM micrographs and EDX spectrum of rusted SAE 1010 steel in aluminum phosphosilicate suspensions. (a) Abraded rusted steel, (b) protective layer (200×), (c) protective layer, other region (140×), (d) protective layer higher magnification (1000×), (e) EDX spectrum of granule like formation, and (f) SEM micrograph of gel like formations.

No red iron spots were observed in the panels exposed to the phosphosilicate solution but panels in the supported electrolyte showed signs of corrosion.

The morphology of the protective layer was revealed after SEM examination. Fig. 5a shows the rusted steel surface after manual brushing and abrading with emery paper No. 100. Abrading lines can be appreciated. The protective layer formed onto the panels after being in contact with the aluminum phosphosilicate suspension was constituted by a uniform film and zones with a smoother texture and dark spots (Fig. 5b and c). Fig. 5d revealed the existence of other morphologies such as granule-like formations and plates. The protective layer was mainly composed by phosphatized iron oxihydroxides. The composition of the granules was basically iron oxihydroxides with low P (2.81%), Al (1.13%) and Si (0.81%) contents. The oxihydroxides content in the rest of the formations was significantly lower with a strong contribution of the base metal, as it could be deduced from the low surface O content. Finally, the presence of gels formed by phosphatized iron oxihydroxides was detected (Fig. 5e); being the P content ~16.1%, and the Al one ~5.2%. The presence of silica in the film grown on the base metal is desirable because it restrains the corrosion process by diminishing the diffusion coefficients of iron ions [49]. However, in all cases, the content of Si was rather low (0.11%).

The composition of the protective layer generated by chromate was extensively studied in previous research. It was found to be constituted by iron oxides stabilized by chromium ions [50,51].

Steel corrosion rate in the presence of the pigment was, in general, somewhat higher; particularly after 4 h of exposure (Table 2). This last aspect will show that aluminum phosphosilicate pigment is not a passivating one but it was active in regard to the dissolution of rusted steel. Corrosion rate did not change significantly after 6 h and decreased after 1 day after of immersion in the electrolyte medium. This can be attributed to the structure of the film formed on the electrode composed by the original oxides and

Table 2
Rusted steel corrosion rate.

Electrolyte	2 h	4 h	6 h	24 h
1	82.7 μA cm^{-2}	93.7 μA cm^{-2}	0.10 mA cm^{-2}	70.8 μA cm^{-2}
2	0.19 mA cm^{-2}	0.16 mA cm^{-2}	0.18 mA cm^{-2}	71.8 μA cm^{-2}

References: Electrolyte 1: normally aerated 0.1 M NaCl, stirred at 300 rpm.
Electrolyte 2: aluminum phosphosilicate suspension in normally aerated 0.1 M NaCl, stirred at 300 rpm.

phosphatized oxides. If pH was raised to 7.0, steel corrosion rate significantly decreased till ~7% of its original value. This property of aluminum phosphosilicate was attributed to the protonation of the silica phase at the precipitation pH (3.5).

3.4. Characterization of the protective layer formed beneath the primer by SEM

The metallic surface under the chromate primer was covered with a uniform base film with micrometric agglomerates grown on it (Fig. 6a). Globular formations contained, basically, iron oxihydroxides with low Cr (0.85%) and Zn (5.14%) contents. The base film was examined with a higher magnification and presented cavities with smaller particles (Fig. 6b). The composition of the base film in these cavities was slightly different because it contained higher amounts of Cr (1.67–3.24%) and P ~3.6%. The zinc content was relatively high and varied between 11.6% and 21.8%. The presence of zinc in the protective film was considered beneficial because it polarizes cathodic areas by precipitating zinc hydroxide, thus inhibiting oxygen discharge [52]. Globular formations in Fig. 6b were constituted principally by iron oxihydroxides with smaller concentration of Cr (0.30%) and zinc (~1.1%). Phosphorous could not be detected due to the overlapping of the peak corresponding to P with the peak of Au.

The protective film formed under the primer containing aluminum phosphosilicate was constituted by gel particles accumulations (Fig. 6c). The gels were phosphatized iron oxihydroxides (Fe: ~52%); the phosphate content was rather high (P: 9.75%) and the film contained Si (1.3%). The P content increased in the globular formations (~15%) while the Fe content decreased (~35%). The presence of silicon was reported to be beneficial because it restrains the corrosion process by significantly diminishing the diffusion coefficient of iron ions through the protective film [49].

3.5. Accelerated tests and electrochemical essays on painted panels

The best anti-corrosion behavior in the salt spray test was observed when the metal substrate was primed with the formulation containing aluminum phosphosilicate (Table 3). The panels painted with the wash primer containing chromate failed after 2550 h as the control panels did. In change, panels coated with the phosphate primer maintained a good qualification still after 2860 h of exposure. Adhesion of both wash primers was satisfactory in the whole test period of each set of panels.

Polarization curves of primed panels revealed that currents were lower in the case of primed metals with respect to the bare metallic substrate (Fig. 7). This fact may be attributable to the barrier effect due to the applied wash-primer. As time elapsed, steel dissolution took place at higher potentials, thus revealing the inhibition of metal dissolution by the primer.

Corrosion potentials remain displaced towards more positive values (>−100 mV vs. SCE) for at least 100 days of testing, thus indicating that the base metal remained protected (Fig. 8). During this period the corrosion potential of the control panel, without priming, showed some fluctuations towards more negative values and, finally, after 111 days, it moved to more negative values revealing the beginning of the corrosion process. The corrosion

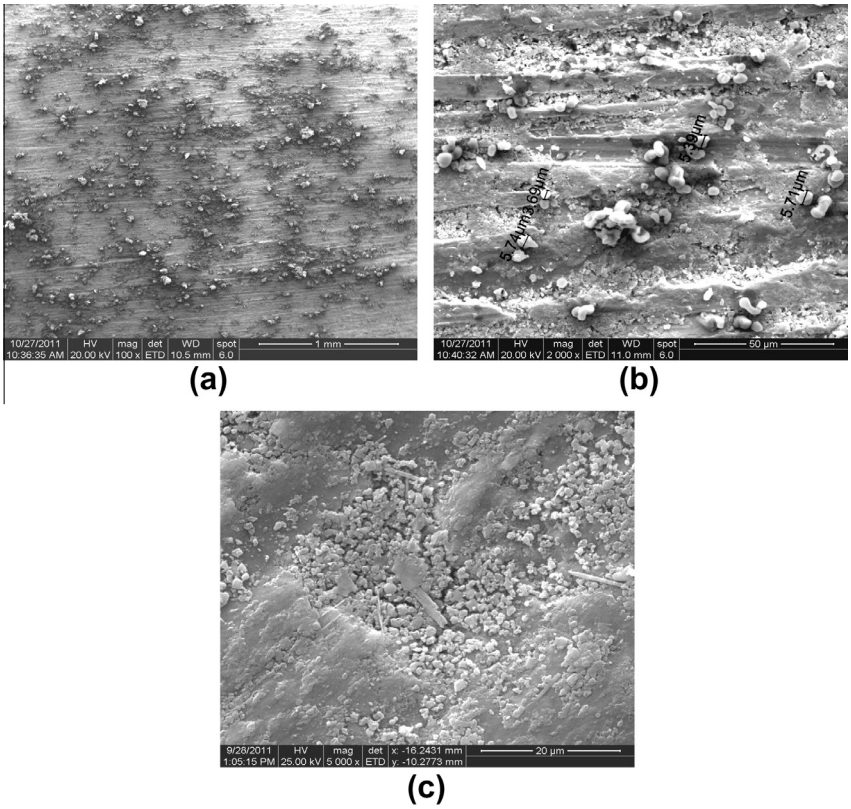

Fig. 6. SEM Morphology and EDX spectrum of the protective layer formed on steel, under the primer film. (a–c) Chromate primer, (d–e) aluminum phosphosilicate primer.

Table 3
Rusting degree (ASTM D 610) of rusted steel panels, primed and coated with the alkyd system, in the salt spray test (ASTM B 117).

Primer	Exposure time (h)							
	1000	1400	1780	1900	2190	2550	2860	3050
Zinc tetroxychromate	10	10	9	8	7	6	–	–
Aluminum phosphosilicate	10	10	10	10	9	8	8	6
Control panel	10	10	8	7	7	6	–	–

Rusting degree (ASTM D 610)

Rusting degree	10	9	8	7	6	5	4	3	2	1
% rusted area	No rust	0.03	0.1	0.3	1	3	10	16	33	50

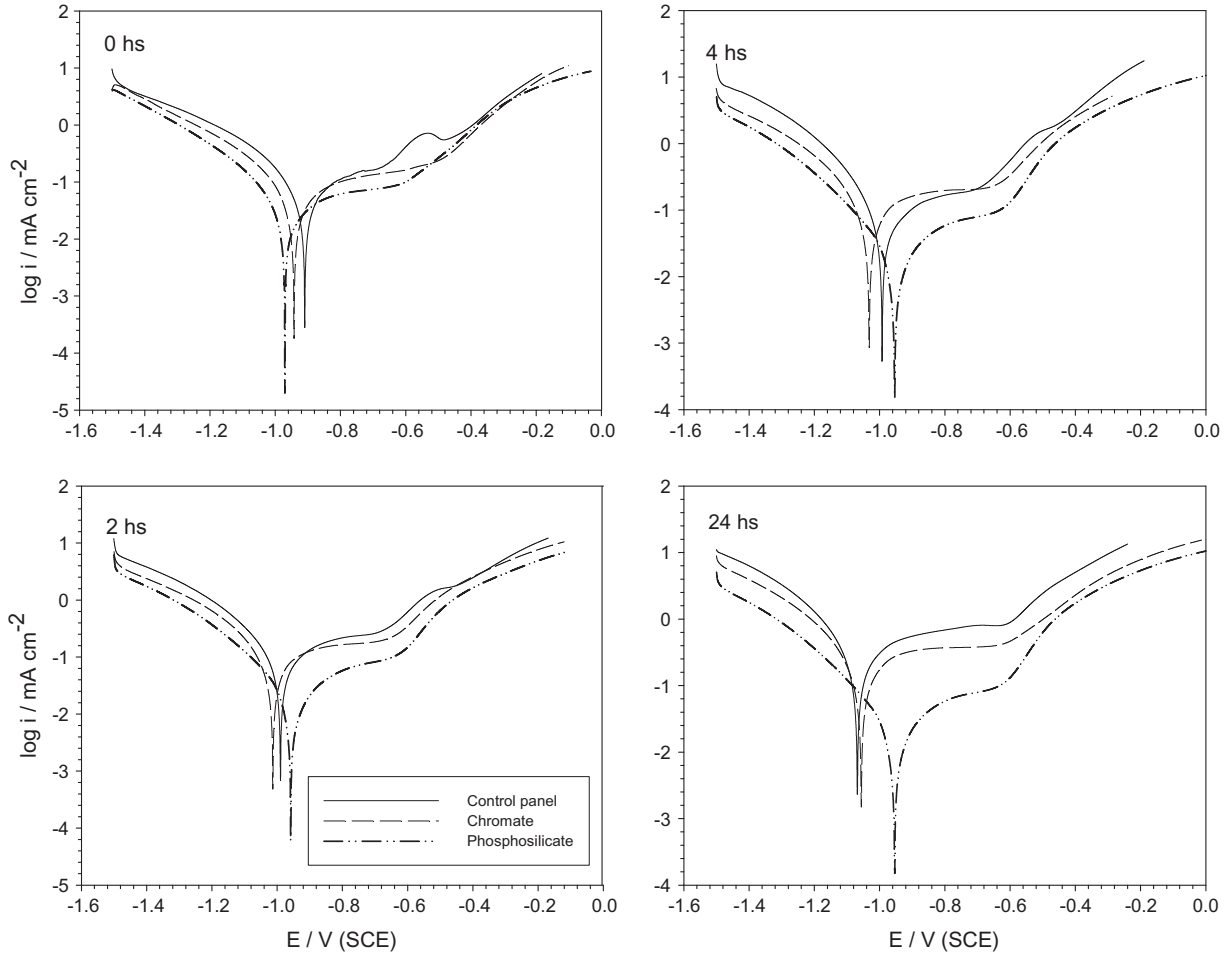

Fig. 7. Polarization curves of rusted SAE 1010 steel in 0.1 M NaCl. Scan rate 1 mV s^{-1}.

potential of panels containing the chromate based primer exhibited characteristic values corresponding to protected steel throughout the assay. Instead, panels containing the wash primer formulated with aluminum phosphosilicate were protected for ~200 days. After 227 days of immersion, the corrosion potential of these panels dropped off but they showed a marked tendency to repassivation as time went on. Taking into account that all panels have the same alkyd coating system, it is concluded that these primers significantly improve the behavior of painted rusted steel.

Impedance spectra give useful information concerning the evolution of both, the organic coating protective properties and the kinetics of the underlying steel corrosion process, as a function of the immersion time in the selected electrolyte. Many processes, such as the dynamic nature of the membrane barrier effect, the pigments protective action, and changes in the disbonded area, are responsible of the variations of the coated steel/electrolyte impedance. The point of view adopted in this paper was that of Amirudin and Thierry [53] in the sense that visual observation of the spectra could not indicate the exact number of time constants involved in the degradation of the organic coating subjected to a corrosive environment, in change the number of these constants must be determined by data analysis rather than by visual observation of spectra.

Fortunately, appropriate equivalent circuits have been proposed to describe the behavior of painted metals (Fig. 9a–d); these circuits were discussed previously by several authors [54–63]. Experimental impedance data are usually fitted with non-linear least squares algorithms, involving the transfer function derived from the equivalent circuit models, to obtain circuit parameters [64–67].

The impedance of a high-quality, non-defective organic coating, is that of a dielectric capacitor with a frequency dependence expressed by the following equation:

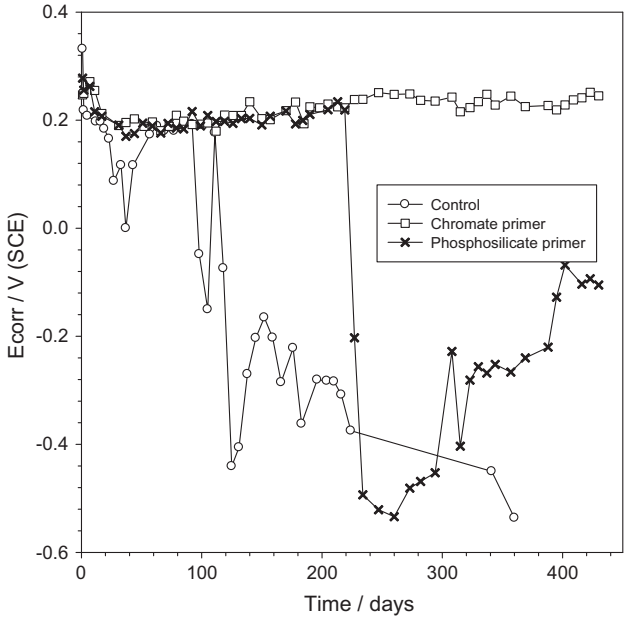

Fig. 8. Corrosion potential of painted panels as a function of time.

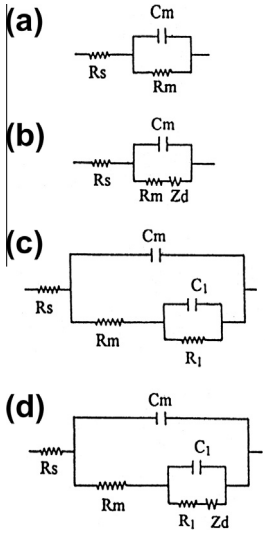

Fig. 9. Equivalent circuits to fit EIS experimental data. Rs: uncompensated resistance, Rm: ionic resistance; Cm: coating capacitance; R1: charge transfer resistance, C1: double layer capacitance, Zd: Warburg impedance. Corrosion potential of painted panels as a function of time.

$$Zc = -j/Wc$$

However, as the coating degrades, an in-phase component develops as a result of shorting the organic coating capacitance with a parallel resistor. This resistor represents the development of ionic conducting paths which may occur through microscopic pores or virtual pores defined by low cross-linking regions in the polymer with concomitant high ionic transport. This model has essentially been proposed by Brasher and Nurse [59], Kendig and Leidheiser [60,61], Kendig and Scully [55], Mansfeld and Kendig [62] and Beaunier and co-workers [63]. Thus, Rs represents the electrolyte resistance between the reference and working (coated steel) electrodes, Rm the resistance to the ionic flux through paths short-circuiting the paint film, and Cm the dielectric capacitance of the intact part of the same film (Fig. 9A). Zd, the mass transfer (Warburg) impedance could appear revealing the mass transport of corroding species (Fig. 9b).

Once the permeating and corrosion-inducing chemicals (water, oxygen and ionic species) reach the electrochemically active areas of the substrate, particularly the bottom of the paint film pores, metallic corrosion takes place and its associated parameters, the double layer capacitance (C_1) and the charge transfer resistance (R_1) can be obtained from the fitting procedure. It is important to remark that R_1 and C_1 values vary inverse and directly, respectively, and with the size of the attacked metallic area. There is almost a unique opinion that a polymer coated metal is represented by the circuit in Fig. 9C when water penetrates the coating and reaches the metal. It is also agreed that the general impedance may include the Zd, the mass transfer (Warburg) impedance [53]. Sometimes, when the strength of the bonding forces at the paint/substrate interface are affected (e.g., by wet adhesion), facilitating lateral diffusion of the electrolyte, other processes under and/or within the intact parts of the coating could be graphically and/or numerically separated [68], causing the appearance of an additional time constant (R_2C_2).

Distortions observed in these resistive–capacitive contributions indicate a deviation from the theoretical models due to either lateral penetration of the electrolyte at the steel/paint interface (usually started at the base of intrinsic or artificial coating defects), underlying steel surface heterogeneity (topological, chemical composition, surface energy) and/or diffusional processes that could take place along the test [69]. Since all these factors cause the impedance/frequency relationship to be non-linear, they are taken into consideration by replacing the capacitive components (C_i) of the equivalent circuit transfer function by the corresponding constant phase element Q_i (CPE), thus obtaining a better data fitting [70]. The CPE is defined by the following equation:

$$Z = \frac{(j\omega)^{-n}}{Y_0} \tag{1}$$

where Z is the impedance of the CPE ($Z = Z' + Z''$) (Ω), j is imaginary number ($j^2 = -1$), ω = angular frequency (rad), n = CPE power ($n = \alpha/(\pi/2)$ (dimensionless), α = constant phase angle of the CPE (rad), Y_0 - = part of the CPE independent of the frequency (Ω^{-1}).

The accuracy of the fitting procedure was measured by the χ^2 parameter obtained from the difference between experimental and fitted data; the most probable circuit was selected providing that $\chi^2 < 10^{-4}$.

In the present work, the fitting process was mainly performed using the phase constant element Q_i instead of the dielectric capacitance C_i. However, this last parameter was used in the plots in order to facilitate results visualization and interpretation.

From the examination of Bode's plots it must be concluded that the impedance modulus was initially high (>$10^7\ \Omega\ cm^2$) for the three studied systems (Figs. 10–12), thus indicating the existence of an acceptable barrier effect. The impedance of the non-primed panels descended sensibly after 138 days of immersion (Fig. 10a). In change the impedance of primed panels maintained rather high during 213 days (Figs. 11a, 12a), being that of the panels primed with the chromate formulation (Fig. 11a) slightly lower than the impedance of steel coated with the wash primer containing aluminum phosphosilicate (Fig. 12a). This fact revealed that the application of the wash-primer added an additional protection to the metal substrate, independently of the inhibitive pigment. No significant differences were found between both types of anticorrosion pigment. The values obtained for the phase angle indicated a resistive–capacitive behavior. As it was said before,

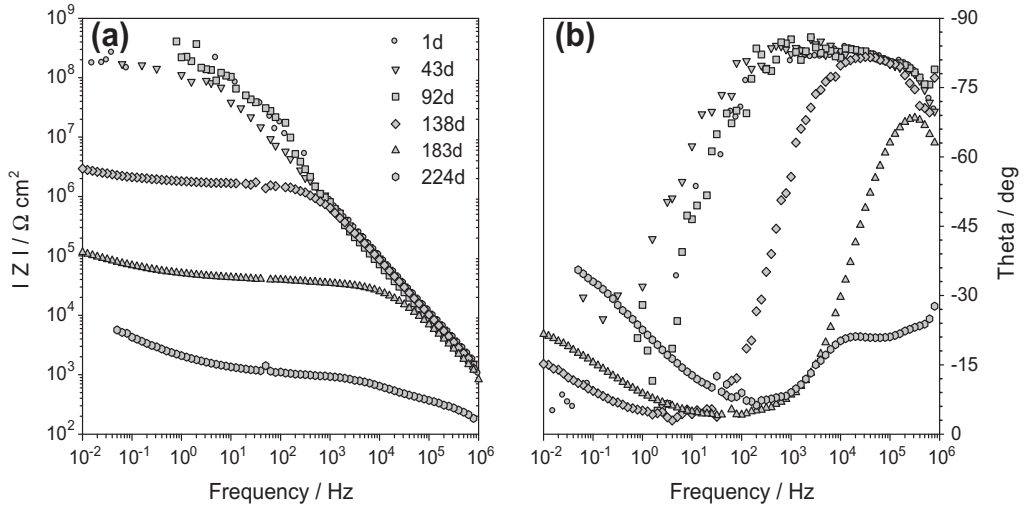

Fig. 10. Bode's plots of non-primed rusted SAE 1010 steel, coated with alkyd system, as a function of the immersion time in 3% NaCl. (a) Impedance modulus, (b) phase angle.

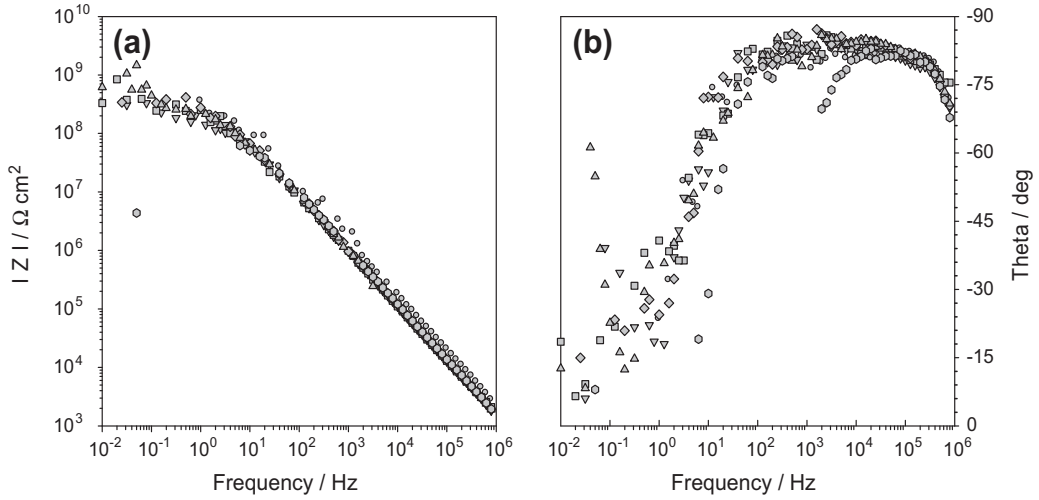

Fig. 11. Bode's plots of SAE 1010 rusted steel primed with the chromate formulation and coated with the alkyd system, as a function of the immersion time in 3% NaCl. (a) Impedance modulus, (b) phase angle.

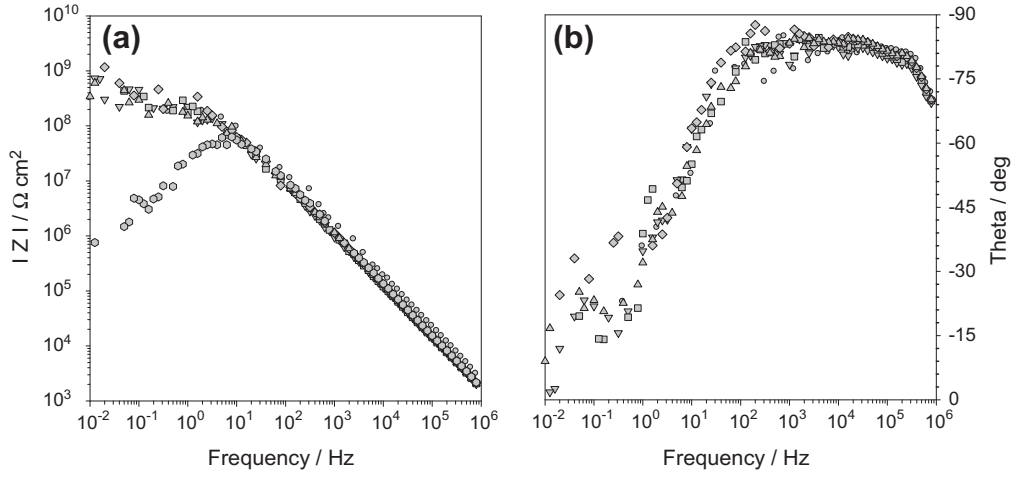

Fig. 12. Bode's plots of SAE 1010 rusted steel primed with the phosphosilicate formulation and coated with the alkyd system, as a function of the immersion time in 3% NaCl. (a) Impedance modulus, (b) phase angle.

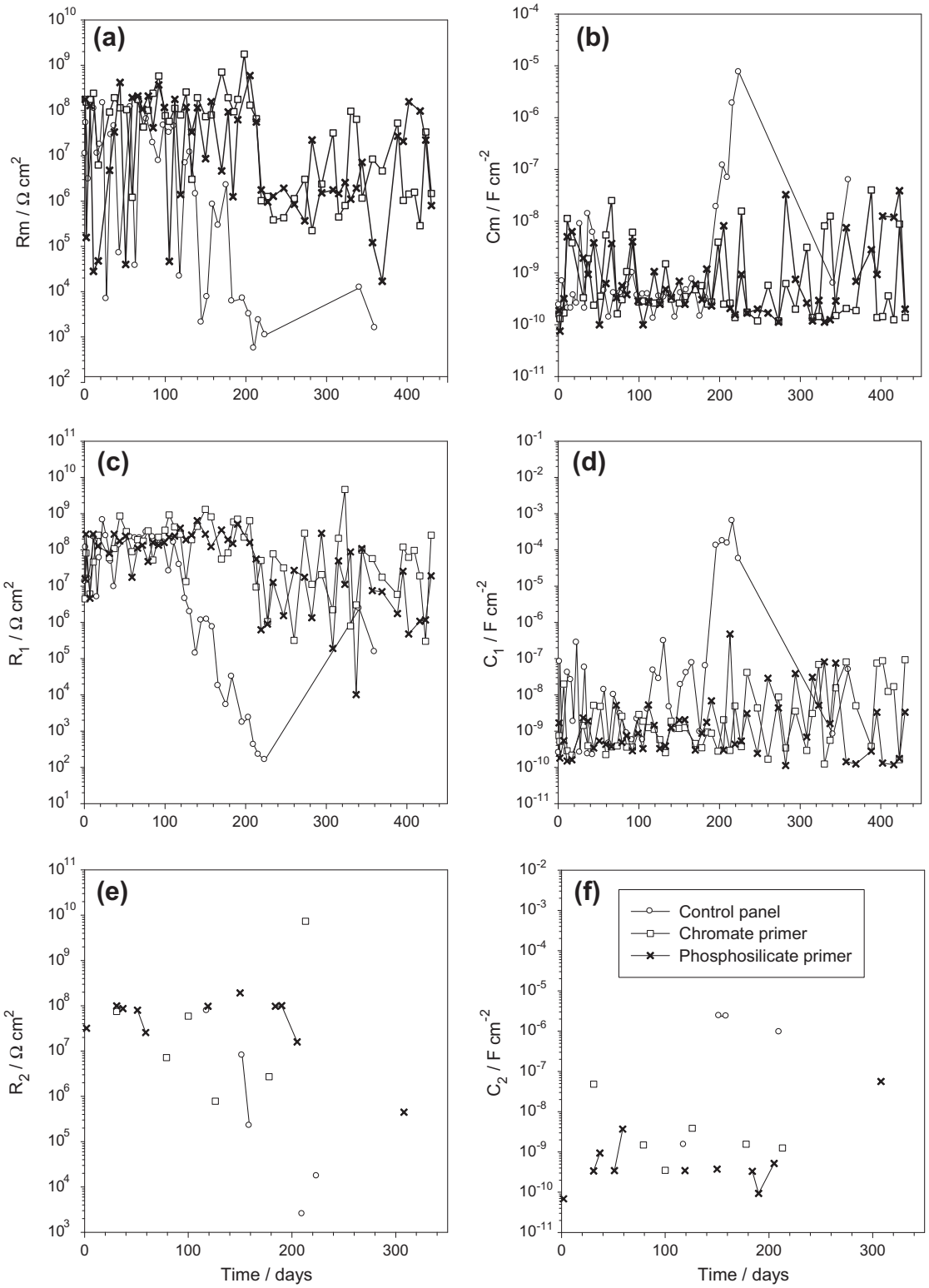

Fig. 13. Variation of the electrochemical parameters, obtained from EIS measurements, corresponding to painted rusted steel. (a) Ionic resistance, (b) dielectric capacitance of the intact part of the coating, (c) charge transfer resistance, (d) electrochemical double layer capacitance, (e) resistance of the localized corrosion products layer, (f) capacitance of the localized corrosion products layer.

the best procedure to find out the exact number of constant times is by fitting experimental data with appropriate models.

The paint systems containing both wash primers had an appreciable barrier effect (Rm > 10^6 Ω cm^2) during ~213 days while this effect was lost after 111 days of immersion in the case of the control panels (Fig. 13a and b). The ionic resistance values oscillated during the test period due, probably, to temporary pore plugging by corrosion products. The capacity of the paint film (Cm) varied

concomitantly, being the control panel (without priming) more prone to degradation as it could be deduced from the increased capacity values. No significant differences were observed among the primed panels.

The charge transfer resistance of primed panels was, as a general rule, higher than $10^6\ \Omega\ cm^2$, this fact would be pointing out the inhibition of the corrosion process. The charge transfer resistance (R_1) of the control panel begun to decrease after 125 days of immersion, exhibiting a slight tendency to repassivation. The values of the parameter C_1 were relatively low suggesting that the electrochemically active area was small and variable, as it could be appreciated by the observed fluctuations. Most values were below 10^{-8} F cm^{-2}; but the highest values corresponded to the control panels (Fig. 13c and d).

The appearance of a third time constant (R_2C_2) was associated with localized corrosion processes which differentiate from the most generalized oxidation process. These processes may involve, for example, corrosion in delaminated areas with subsequent formation of a corrosion products layer. This type of corrosion was, generally, inhibited in the case of the primed panels as it may be deduced from the recorded values of R_2. The affected areas were small as it could be deduced from the values obtained for C_2 which were below 10^{-8} F cm^{-2}. These processes stopped after 210 days of immersion and they did not relax continuously that was why points are not always joined in Fig. 13e and f. They appeared at certain definite times and then disappear; probably due to passivation of the corrosion zone.

These electrochemical measurements revealed that this rather simple low thickness paint system can afford a protection degree similar to that obtained with self-priming systems [33,34]. As aluminum phosphosilicate is acidic in nature, it can be used with other acid binders to formulate similar primers. Its anti-corrosion performance was also proved on hot dip galvanized steel [71].

4. Conclusion

Rusted steel may be painted in a satisfactory way employing the eco-friendly wash-primers developed in this research. The anti-corrosion behavior of both wash-primers was similar, this fact would be indicating that the replacement of chromate by aluminum phosphosilicate is possible maintaining good performance.

Aluminum phosphosilicate was synthesized in such a way that it was acidic in nature and fully compatible with the wash primer formulation. The tested formulation was capable of phosphating the existing oxides on the steel surface. The employment of this pigment is not only restricted to the formulation proposed in this research but it may be also employed with other binders checking its compatibility with the rest of the formulation, particularly the binder.

References

[1] D. de la Fuente, M. Bohm, C. Houyoux, M. Rohwerder, M. Morcillo, The settling of critical levels of soluble salts for painting, Prog. Org. Coat. 58 (2007) 23–32.
[2] D. de la Fuente, J. Simancas, M. Morcillo, Effect of variable amounts of rust at the steel/paint interface on the behavior of anticorrosive paint systems, Prog. Org. Coat. 46 (4) (2003) 241–249.
[3] C.I. Elsner, E. Cavalcanti, O. Ferraz, A.R. Di Sarli, Evaluation of the surface treatment effect on the anticorrosive performance of paint systems on steel, Prog. Org. Coat. 48 (1) (2003) 50–62.
[4] B.A. Scott, R.E. Shaw, H.G. Cole, Chemical conversion coatings, in: L.L. Shreir (Ed.), Corrosion Control, vol. II, Newnes, Butterworth, London, 1976, pp. 1–42 (Chapter 16).
[5] S. Paul, Surface preparation and paint application, in: S. Paul (Ed.), Surface Coatings. Science and Technology, second ed., John Wiley and Sons, England, 1996, pp. 477–510 (Chapter 6).
[6] J.M. Waldie, Conversion Coatings, in: J.M. Waldie, Chairman Textbook Committee, Surface Coatings, Vol. II: Paints and Their Applications, OCCA Australia, England, 1984, pp. 578–588.
[7] U.R. Evans, C.A.J. Taylor, Mechanism of atmospheric rusting, Corros. Sci. 12 (1972) 227–246.
[8] M. Stratmann, H. Streckel, On the atmospheric corrosion of metals which are covered with thin electrolyte layers—II. Experimental results, Corros. Sci. 30 (1990) 697–714.
[9] A. Kuch, Investigations of the reduction and re-oxidation kinetics of iron(III) oxide scales formed in waters, Corros. Sci. 28 (1988) 221–231.
[10] M. Stratmann, J. Muller, The mechanism of the oxygen reduction on rust-covered metal substrates, Corros. Sci. 36 (1994) 327–359.
[11] M. Stratmann, K. Hoffmann, *In situ* Möβbauer spectroscopic study of reactions within rust layers, Corros. Sci. 29 (1989) 1329–1352.
[12] M. Yamashita, H. Miyuki, Y. Matsuda, H. Nagano, T. Misawa, The long term growth of the protective rust layer formed on weathering steel by atmospheric corrosion during a quarter of a century, Corros. Sci. 36 (1994) 283–299.
[13] M. Stratmann, K. Bohnenkamp, T. Ramchandran, The influence of copper upon the atmospheric corrosion of iron, Corros. Sci. 27 (1987) 905–926.
[14] I. Suzuki, Y. Hisamatsu, N. Masuko, Electrochemical properties of iron rust, Corros. Sci. 19 (1979) 521–535.
[15] T. Kamimura, M. Stratmann, The influence of chromium on the atmospheric corrosion of steel, Corros. Sci. 43 (2001) 429–447.
[16] T.K. Ross, R.A. Francis, The treatment of rusted steel with mimosa tannin, Corros. Sci. 18 (4) (1978) 351–361.
[17] J.A. Jaén, E.Y. Araúz, J. Iglesias, Y. Delgado, Reactivity of tannic acid with common corrosion products and its influences on the hydrolysis of iron in alkaline solutions, Hyperfine Interact. 148–149 (2003) 199–209.
[18] J.A. Jaén, L. González, A. Vargas, G.Y. Olave, Gallic acid, ellagic acid and pyrogallol. Reaction with metallic iron, Hyperfine Interact. 148–149 (2003) 227–235.
[19] J. Gust, J. Suwalski, Use of Mössbauer spectroscopy to study reaction products of polyphenols and iron compounds, Corrosion 50 (5) (1994) 355–365.
[20] J. Iglesias, E. García de Saldaña, J.A. Jaén, On the tannic acid interaction with metallic iron, Hyperfine Interact. 134 (2001) 109–114.
[21] S. Martinez, I. Štern, Ferric-Tannate formation and anticorrosive properties of mimosa tannin in acid solutions, Chem. Biochem. Eng. Q 13 (4) (1999) 191–199.
[22] S. Martinez, I. Štern, Inhibitory mechanism of low-carbon steel corrosion by mimosa tannin in sulphuric acid solutions, J. Appl. Electrochem. 31 (9) (2001) 973–978.
[23] S. Martinez, I. Štern, Thermodynamic characterization of metal dissolution and inhibitor adsorption processes in the steel/mimosa tannin/sulfuric acid, Appl. Surf. Sci. 199 (1–4) (2002) 83–89.
[24] S. Martinez, Inhibitory mechanism of mimosa tannin using molecular modeling and substitutional adsorption isotherms, Mater. Chem. Phys. 77 (1) (2002) 97–102.
[25] O.R. Pardini, J.I. Amalvy, A.R. Di Sarli, R. Romagnoli, V.F. Vetere, Formulation and testing of a water-borne primer containing chestnut tannin, J. Coat. Technol. 73 (913) (2001) 99–106.
[26] S. Hornus Sack, R. Romagnoli, V.F. Vetere, C.I. Elsner, O. Pardini, J.I. Almalvy, A.R. Di Sarli, Evaluation of steel/primer based on chestnut tannin/paint film systems by EIS, J. Coat. Technol. 74 (926) (2002) 63–69.
[27] G. Matamala, W. Smeltzer, G. Droguett, Comparison of steel anticorrosive protection formulated with natural tannins extracted from acacia and from pine bark, Corros. Sci. 42 (8) (1994) 1351–1362.
[28] A. Jaén, J. de Obaldía, M.V. Rodríguez, Application of Mössbauer spectroscopy to the study of tannins inhibition of iron and steel corrosion, Hyperfine Interact. 202 (1–3) (2011) 25–38.
[29] Afidah.A. Rahim, E. Rocca, J. Steinmetz, M.J. Kassim, R. Adnan, M. Sani Ibrahim, Mangrove tannins and their flavanoid monomers as alternative steel corrosion inhibitors in acidic medium, Corros. Sci. 49 (2) (2007) 402–417.
[30] A.A. Rahim, E. Rocca, J. Steinmetz, M. Jain Kassim, Inhibitive action of mangrove tannins and phosphoric acid on pre-rusted steel via electrochemical methods, Corros. Sci. 50 (2008) 1546–1550.
[31] Collazo, X.R. Nóvoa, C. Pérez, B. Puga, EIS study of the rust converter effectiveness under different conditions, Electrochim. Acta 53 (25) (2008) 7565–7574.
[32] L.M. Ocampo, I.C.P. Margarit, O.R. Mattos, S.I. Córdoba-de-Torresi, F.L. Fragata, Performance of rust converter based in phosphoric and tannic acids, Corros. Sci. 46 (6) (2004) 1515–1525.
[33] D.D.N. Singh, Dhrubo Bhattacharya, Performance and mechanism of action of self-priming organic coating on oxide covered steel surface, Prog. Org. Coat. 67 (2) (2010) 129–136.
[34] D.N. Singh, Dhrubo Bhattacharya, Performance and mechanism of action of self-priming organic coating on oxide covered steel surface, Prog. Org. Coat. 68 (1–2) (2010) 62–69.
[35] C. Wilson, D. Wilson, Comprehensive Analytical Chemistry, Elsevier Publishing Company, Amsterdam, 1960.
[36] R.B. Fischer, D.G. Peters, Quantitative Chemical Analysis, W.B. Saunders Co., Mexico, 1968.
[37] M. Stern, A.L. Geary, Electrochemical polarization: I. A theoretical analysis of the shape of polarization curves, J. Electrochem. Soc. 104 (1) (1957) 56–61.
[38] S. Wolynec, Determinação da taxa de corrosão e de outros parâmetros", in: S. Wolynec (Ed.), Técnicas Eletroquimicas en Corroção, Editora da Universidade de São Paulo, Brasil, 2003, pp. 95–114.
[39] F.J. Rodríguez Gómez, Técnicas electroquímicas de corriente directa para la medición de la velocidad de corrosion. Resistencia a la polarización, in: J. Genescá LLongueras (Ed.), Técnicas Electroquímicas Para el Estudio de la

Corrosion, Laboratorio de Corrosión de la Facultad de Química de la UNAM, México, pp. 1–9 (Capítulo 2).
[40] Butvar. Polyvinyl butiral resin. Properties and uses. Publication No. 2008084E, Coatings performance materials by SOLUTIA, <http://www.butvar.com>.
[41] G.W. Walter, A review of impedance plot methods used for corrosion performance analysis of painted metals, Corros. Sci. 26 (9) (1986) 681–703.
[42] B.A. Boukamp, Report CT88/265/128, CT89/214/128, University of Twente, The Netherlands, 1989.
[43] D. Veselý, V. Jašková, Efficiency of anticorrosive pigments based on metal phosphates, Transfer Inovácií 15 (2009) 151–154.
[44] B.N. Rupa, H.M. Bhavnagary, Preparation of precipitated metal silicophosphates. Part-I. Low temperature synthesis of aluminum silicophospahtes, J. Indian Chem. Soc. (1987) 389–392.
[45] B. Smith, Inorganic Compounds, in Infrared Spectral Interpretation. A Systematic Approach, CRC Press, USA, 1999. Capítulo 7, pp. 168–175.
[46] D.G. Anderson, J.K. Duffer, J.M. Julian, R.W. Scott, T.M. Sutliff, M.J. Vaickus, The Infrared Spectroscopy Committee of the Chicago Society for Coatings Technology, Pigments, Extenders and Other Crystalline Materials in: An Infrared Spectroscopy Atlas for the Coating Industry, USA, vol. I, Chapter IX, 1980, p. 111.
[47] U. Schwertman, R.M. Cornell, Iron Oxides in the Laboratory: Preparation and Characterization, Wiley-VCH, Deutschland, 2000 (Chapters 5–14).
[48] Marijan Gotic, Svetozar Music, Mössbauer, FT-IR and FE SEM investigation of iron oxides precipitated from $FeSO_4$ solutions, J. Mol. Struct. 834–836 (2007) 445–453.
[49] M.J. Bennet, M.R. Houlton, R.W.M. Hawes, The improvement by a CVD silica coating of the oxidation behavior of a 20% Cr/25% Ni niobium stabilized stainless steel in carbon dioxide, Corros. Sci. 22 (2) (1982) 111–113.
[50] M.W. Kendig, A.J. Davenport, H.S. Isaacs, The mechanism of corrosion inhibition by chromate conversion coatings from X-ray absorption near edge spectroscopy (XANES), Corros. Sci. 34 (1) (1993) 41–49.
[51] M.J. Pryor, M. Cohen, The inhibition of the corrosion of iron by some anodic inhibitors, J. Electrochem. Soc. 100 (5) (1953) 203–215.
[52] Z. Szklarska-Smialowska, R.W. Staehle, Ellipsometric study of the formation of films on iron in orthophosphate solution, J. Electrochem. Soc. 121 (11) (1974) 1393–1401.
[53] A. Amirudin, D. Thierry, Application of electrochemical impedance spectroscopy to study efficiency of anticorrosive pigments in epoxy–polyamide resin, Br. Corros. J. 30 (2) (1995) 128–134.
[54] F. Mansfeld, Recording and analysis of AC impedance data for corrosion studies. Background and methods of analysis, Corrosion 36 (5) (1981) 301–307.
[55] M. Kendig, J. Scully, Basic aspects of electrochemical impedance, application for the life prediction of organic coatings on metals, Corrosion 46 (1990) 22–29.
[56] T. Szauer, Impedance measurements for the evaluation of protective nonmetallic coatings, Prog. Org. Coat. 10 (2) (1982) 171–183.
[57] S. Skale, V. Doleček, M. Slemnik, Electrochemical impedance studies of corrosion protected surfaces covered with epoxy polyamide coating system, Prog. Org. Coat. 62 (2008) 387–392.
[58] A. Miszczyk, H. Szalinska, Laboratory evaluation of epoxy coatings with an adhesion promoter by impedance, Prog. Org. Coat. 25 (1995) 357–363.
[59] D. Brasher, T.J. Nurse, Electrical Measurements of immersed paint coatings on metal. II. Effect of osmotic pressure and ionic concentration of solution on paint breakdown, J. Appl. Chem. 9 (1959) 96–105.
[60] H. Leidheiser Jr., M.W. Kendig, Mechanism of corrosion of polybutadiene-coated steel in aerated sodium chloride, Corrosion 32 (1976) 69–76.
[61] M.W. Kendig, H. Leidheiser, Electrical properties of protective polymer coatings as related to corrosion of the substrate, J. Electrochem. Soc. 123 (7) (1976) 982–989.
[62] F. Mansfeld, M. Kendig, in: C. Haynes, R. Baboian (Eds.), Electromechanical Impedance Tests for Protective Coatings, ASTM Publication STP 866, Philadelphia, PA, 1985, pp. 122–142.
[63] L. Beaunier, I. Epelboin, J.C. Lestrade, H. Takenouti, Etude electrochimique, et par microscopie electronique a balayage, du fer recouvert de peinture, Surf. Technol. 3 (1976) 237–254.
[64] O. Ferraz, E. Cavalcanti, A.R. Di Sarli, The characterization of protective properties for some naval steel/polymeric coatings/3%NaCl solution systems by EIS and visual assessment, Corros. Sci. 37 (8) (1995) 1267–1280.
[65] P.R. Seré, D.M. Santágata, C.I. Elsner, A.R. Di Sarli, The influence of the meted of application of paint on the corrosion of the substrate as assessed by ASTM and electrochemical methods, Surf. Coat. Int. 3 (1998) 128–134.
[66] D.M. Santágata, P.R. Seré, C.I. Elsner, A.R. Di Sarli, Evaluation of the surface treatment effect on the corrosion performance of paint coated carbon steel, Prog. Org. Coat. 33 (1998) 44–54.
[67] P. Seré, R.A. Armas, C.I. Elsner, A.R. Di Sarli, The surface condition effect on adhesion and corrosion resistance of carbon steel/chlorinated rubber/artificial sea water systems, Corros. Sci. 38 (6) (1996) 853–866.
[68] C. Gabrielli, M. Keddam, O.R. Mattos, H. Takenouti, Charge transfer resistance measurements by galvano-static double pulse and impedance methods, J. Electroanal. Chem. 117 (1981) 147–153.
[69] P.L. Bonora, F. Deflorian, L. Fedrizzi, Electrochemical impedance spectroscopy as a tool for investigating underpaint corrosion, Electrochim. Acta 41 (7–8) (1996) 1073–1082.
[70] J.B. Jorcin, M.E. Orazem, N. Pébère, B. Tribollet, CPE analysis by local electrochemical impedance spectroscopy. <http://oatao.univ-toulouse.fr/643/1/jorcin_643.pdf>.
[71] A.M.P. Simões, R.O. Carbonari, A.R. Di Sarli, B. Del Amo, R. Romagnoli, An environmentally acceptable primer for galvanized steel: formulation and evaluation by SVET, Corros. Sci. 53 (2011) 464–472.